High-spin states of ^{94}Ru and ^{96}Pd

W. F. Piel, Jr.
Physics Department, State University of New York at Stony Brook, Stony Brook, New York 11794

G. Scharff-Goldhaber
Physics Department, Brookhaven National Laboratory, Upton, New York 11973
and Physics Department, Cornell University, Ithaca, New York 14850

C. J. Lister
Physics Department, Brookhaven National Laboratory, Upton, New York 11973
and Schuster Laboratory, University of Manchester, Manchester M139PL, England

B. J. Varley
Schuster Laboratory, University of Manchester, Manchester M139PL, England

(Received 25 March 1983)

High-spin states of neutron-deficient ^{96}Pd up to $J^\pi = 12^+$ have been studied using the ^{60}Ni(^{40}Ca, 2p2nγ)^{96}Pd reaction with 140 MeV ^{40}Ca ions. The weak ^{96}Pd transitions were enhanced and identified by means of multiple-particle γ-ray coincidence techniques. The half-life of the yrast 6^+ state was determined to be 11.7±2.8 ns (0.50 W.u.), in disagreement with a previous measurement, and an additional isomeric half-life of 58±5 ns was detected. Simultaneously, the ^{60}Ni(^{40}Ca,α2pγ)^{94}Ru reaction was observed to populate new high-spin states of ^{94}Ru up to $J \sim 19\hbar$. A cascade of γ-ray transitions between states of ^{94}Ru which may involve the excitation of a $g_{9/2}$ neutron was observed.

NUCLEAR REACTIONS ^{60}Ni(^{40}Ca,2p2nγ)^{96}Pd, ^{60}Ni(^{40}Ca,α2pγ)^{94}Ru, $E = 120$–150 MeV, measured $\sigma_{rel}(E)$, γ-γ coincidence, γ-p, γ-α, γ-n coincidence, n-$\gamma(t)$; ^{66}Zn(^{35}Cl,αp2nγ)^{94}Ru, $E = 165$ MeV, ^{70}Ge(^{32}S,α2p2n)^{94}Ru, $E = 130$ MeV, measured $W(\theta)$; ^{96}Pd, ^{94}Ru deduced levels, J^π, $t_{1/2}$; enriched targets, Ge(Li), Si(SB), NE213 liquid scintillator detectors.
NUCLEAR STRUCTURE ^{96}Pd, ^{94}Ru shell model calculations of level energies and lifetimes.

INTRODUCTION

This paper on the spectrum of the "exotic" nuclide $^{96}_{46}Pd_{50}$ brings to successful conclusion a series of attempts by us to populate and identify its high-spin states by means of heavy-ion reactions. These were undertaken in the course of a study of neutron deficient even-A (Refs. 1–3) and odd-A (Ref. 4) Pd isotopes with $A \leq 104$. There has been recent renewed interest in the $N = 50$ nuclides, spurred by an experimental study of the high-spin states of ^{94}Ru and ^{95}Rh by the Munich group.[5] Moreover, three recent theoretical studies of selected high-spin states of the $N = 50$ nuclides have appeared.[6–8] These nuclides, besides having a single closed shell which facilitates shell model calculations, are of interest because the valence protons in the $g_{9/2}$ (and $p_{1/2}$) orbitals offer a unique opportunity for testing seniority conservation for identical particles. Gloeckner *et al.*[9] had extracted earlier an effective residual interaction from a fit to 45 level energies chosen from ^{90}Zr, ^{91}Nb, ^{92}Mo, ^{93}Tc, and ^{94}Ru.

One goal of the present study was the identification of high-spin states of exotic ^{96}Pd in order to explore further the extent of seniority nonconservation. A preliminary report of this work[10] assigned a γ-ray cascade to ^{96}Pd on the basis of γ-ray excitation functions observed for ^{32}S + ^{68}Zn, ^{32}S + ^{70}Ge, and ^{16}O + ^{84}Sr bombardments. This cascade was, however, subsequently found to occur instead in ^{93}Tc.[11] Therefore our primary purpose was the assignment of the correct cascade to ^{96}Pd. A careful evaluation of the residual nuclides populated in the three bombardments indicated that the majority have an atomic number Z which is at least 2 less than that of the compound nuclide produced by fusion—i.e., there is a propensity for charged particle evaporation over neutron evaporation in these reactions. This experience coupled with detailed nuclear evaporation calculations suggested that the use of the ^{60}Ni(^{40}Ca,2p2nγ)^{96}Pd reaction would offer greatly improved prospects for identifying and studying ^{96}Pd. In particular, it is of interest to see whether or not the ^{96}Pd $8^+ \rightarrow 6^+$ transition occurs with a strength similar to that found both in ^{90}Zr (2.5 W.u.) and ^{92}Mo (1.3 W.u.) rather than the extreme retardation previously found to occur in ^{94}Ru (3.4×10^{-3} W.u.). It was found necessary to employ particle–gamma-ray coincidence techniques in order to enhance and identify the weak ^{96}Pd transitions. During the course of this work, two studies of ^{96}Pd levels up to $J^\pi = 8^+$ have been reported. Kurcewicz *et al.*[12] have studied the β^+–electron-capture (EC) decay of 5.1 s ^{96}Ag to ^{96}Pd. Their spin-parity assignments are in agreement with our second preliminary report[13,14] as will be shown below. Grawe and Haas[15] have recently measured the g factor and the half-life of the $J^\pi = 8^+$ state as well as the half-life of the 6^+ state. Their value for the g factor is in agreement with expectations based on the nuclear shell model while the 8^+ half-life of 2.22 μs corresponds to a transition strength (0.33 W.u.) which is somewhat weaker than

is found in ^{90}Zr and ^{92}Mo but much stronger than for ^{94}Ru. Their value for the 6^+ half-life is smaller than the value determined from the present experiments as will be shown below. Finally, Aras *et al.*[16] have observed two γ-ray transitions of 124.8 and 499.5 keV following the β^+-EC decay of 2.0 min ^{96}Pd to levels of ^{96}Rh.

EXPERIMENTS

The previous work on the nearby heavier Pd nuclides and the results of nuclear fusion evaporation calculations suggested that the

$$^{60}\text{Ni}(^{40}\text{Ca},2\text{p}2\text{n}\gamma)^{96}\text{Pd}$$

reaction would be suitable for an attempt at identifying transitions in ^{96}Pd as mentioned above. The experiments were performed at the Brookhaven National Laboratory Tandem Van de Graaff facility. The ^{60}Ni target (enriched to 99%) was $\sim$1 mg/cm^2 thick and evaporated onto a $\sim$20 mg/cm^2 layer of lead. A charged-particle neutron—γ-ray coincidence array, installed at the BNL Tandem Laboratory by two of us (C.J.L. and B.J.V.) and displayed in Fig. 1 permitted the nuclidic identification of many of the γ rays produced. The evaporated protons and alpha particles were detected by a silicon surface-barrier [Si(SB)] ΔE-E telescope located at $\theta_{\text{lab}}=0°$ and subtending a solid angle of 0.85 sr. The lead target backing was chosen to be just thick enough to stop the ^{40}Ca beam from striking the telescope while allowing most of the protons and alpha particles to pass through. A two-dimensional display of coincidences between the two Si(SB) detectors produced by ^{40}Ca + ^{60}Ni with $E_{\text{lab}}=140$ MeV is plotted in Fig. 2(b). In Fig. 2(a) are shown the digital gates which were defined during the experiment using a "light pen" interfaced to a computer cathode-ray-tube device. Several γ-ray spectra gated by these regions will be displayed below.

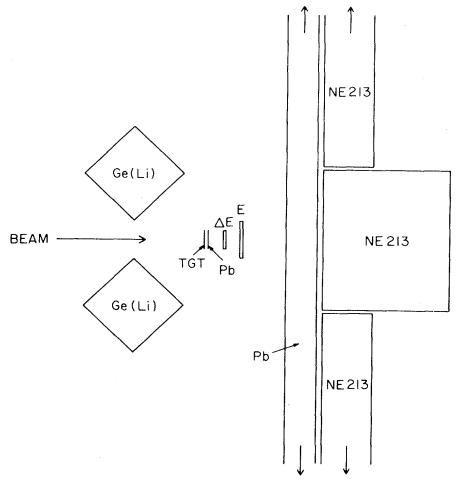

FIG. 1. Diagram of the apparatus used for the γ-ray, multiparticle coincidence experiment. The two Ge(Li) γ-ray detectors are located at $\pm$135°. The Si(SB) ΔE-E telescope was used to detect protons and alpha particles at 0°. A Pb backing stopped the beam. The NE213 liquid scintillator used to detect neutrons was divided into five optically separate parts consisting of four 4 cm thick quadrants and a 15 cm thick central segment. A 3.5 cm thick Pb layer stopped many γ rays from interacting with the liquid scintillator.

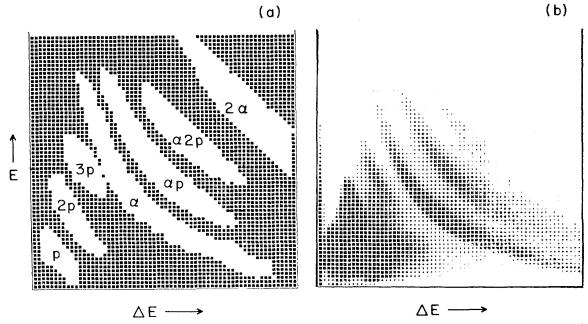

FIG. 2. (a) shows the software gates, labeled by the detected particles used to gate the γ-ray spectra. (b) shows a density plot of data obtained from the Si(SB) ΔE-E telescope using 140 MeV ^{40}Ca + ^{60}Ni. In order to display the relatively weak alpha particle groups, the structure in the more intense proton groups has been washed out.

The evaporated neutrons were detected by an array of five NE213 liquid scintillator detectors centered about $\theta_{\text{lab}}=0°$ and subtending a total solid angle of 3.9 sr. The intensity of γ rays striking the scintillator was reduced by a 3.5 cm thick layer of lead as shown in Fig. 1. The surviving γ ray events were distinguished from neutrons by means of electronic pulse shape discrimination. An inspection of the γ-γ coincidence gates, with the additional requirement of a coincident neutron, revealed no evidence for the transitions of ^{96}Ru which are intensely produced by ^{40}Ca + ^{60}Ni following the evaporation of four protons. This test indicates that the events resulting from γ rays hitting the segments of NE213 were efficiently rejected. The average efficiency for detecting a "second" neutron was 7%. This was determined by comparing, for each of several γ-ray transitions, the ratio of the background-subtracted photopeak intensity in a 2n-gated γ-ray spectrum to that in a 1n-gated spectrum. The use of this method removes the influence of any isomeric levels. This efficiency is smaller than that for detecting only a single neutron, estimated to be 15%, because of the possibility that both neutrons can be detected by the same NE213 segment thereby yielding an apparent single neutron event. Finally, two Ge(Li) γ-ray detectors (each $\sim$85 cm^3) were located at $\theta_{\text{lab}}=\pm 135°$.

Many distinct γ-ray spectra, each with its own gating particles (or none), were recorded during the coincidence experiment. For each Ge(Li) detector a singles spectrum along with spectra gated by various combinations of neutrons, protons, and alpha particles were recorded. These are summarized in Table I where the relative counting rate, for 140 MeV ^{40}Ca ions, in each spectrum is listed. In addition, two event mode recorded (EMR) magnetic tapes were recorded simultaneously for subsequent off-line analysis. One tape provided four parameters for each γ-γ coincidence event: E_{γ_1}, E_{γ_2}, n_ν, and $t_{\gamma\gamma}$, where E_{γ_1} and E_{γ_2} are the Ge(Li) linear signals, $t_{\gamma\gamma}$ is the time difference between them, and n_ν is the number of coincident neutrons (if any). The other tape provided two parameters E_{γ_1} and

TABLE I. The total number of particle–γ-ray coincidences for various gating particles accumulated during a 9.2 h counting interval for ^{40}Ca + ^{60}Ni at 140 MeV as discussed in the text.

Gating particles	Ge(Li) counts ($\times 10^3$)	Gating particles	Ge(Li) counts ($\times 10^3$)
None	308 000	α	3240
n	6480	αn	36.6
2n	41.6	α2n	0.149
p	32 400	αp	445
pn	1180	αpn	4.93
p2n	7.27	αp2n	0.020
2p	4710	α2p	73.9
2pn	140	α2pn	0.714
2p2n	0.756	α2p2n	0.007
3p	545	2α	15.4
3pn	8.47	2αn	0.095
3p2n	0.045	2α2n	0

$t_{n\gamma}$ where $t_{n\gamma}$ is the time difference between the γ ray and the neutron.

In order to obtain information on the multipolarity of the γ-ray transitions of interest, it proved convenient and necessary to utilize γ-ray angular distribution data available from previous experiments performed in this laboratory to study nearby ^{98}Pd (Ref. 3). These data were recorded in two distinct bombardments: (1) ^{35}Cl + ^{66}Zn, $E_{lab}=165$ MeV, and (2) ^{32}S + ^{70}Ge, $E_{lab}=130$ MeV. During each of these experiments an 85 cm^3 Ge(Li) detector was successively positioned at each of eight angles ranging from 60° to 162° with respect to the beam direction for typically 10 min each. The data were normalized to counts above 600 keV in a spectrum from a fixed Ge(Li) detector located at 90° and on the other side of the beam line.

In order to decide on the optimum beam energy to be used to record the ^{40}Ca + ^{60}Ni coincidence data, γ-ray singles spectra were recorded using 120-, 130-, 140-, and 150-MeV bombarding energies. The γ-ray transition intensities, corrected for detector efficiency, obtained for several previously identified nuclides are shown in Fig. 3. These have been normalized to a calculated cross section for the excitation of the lowest $J^\pi=2^+$ state of ^{60}Ni (at 1332.5 keV). The normalization takes into account the estimate that the average energy of the ^{40}Ca ions while transversing the ^{60}Ni layer is about 7 MeV less than the bombarding energy. The calculation of the ^{60}Ni(2^+) excitation function displayed in Fig. 3 was done with CHORK, a coupled channels code, using optical model parameters previously determined from a fit to ^{35}Cl + ^{58}Ni elastic scattering data by Scobel *et al.*[17] A search of the literature indicated that these parameters would probably be the most similar to the analogous ones for the ^{40}Ca + ^{60}Ni system. Also shown in Fig. 3 by the dotted curve are the empirical results of Sikora *et al.*[18] for the total cross section for producing evaporation residues by the ^{40}Ca + ^{60}Ni system. The curve takes into account the present target thickness of about 14 MeV. Using the data depicted in Fig. 3 and taking into account the location of each transition in its level scheme, we have estimated the production cross section for each of nine identifiable nuclides. At 150 MeV, the nuclides and cross sections (in mb) are ^{97}Pd(6), ^{96}Pd(7), ^{96}Rh(45), ^{95}Rh(6), ^{96}Ru(49), ^{95}Ru(21), ^{94}Ru(56), ^{93}Ru(31), and ^{93}Tc(35). The total of 255 mb accounts for (at least) 54% of the total evaporation residue cross section, corrected for target thickness, of 468 mb (at 150 MeV). Calculations using the fusion-evaporation code CASCADE (Ref. 19) suggest that of the remaining 46% of the total cross section, about 15% populates low-spin states (and, therefore, does not contribute to yrast cascades) while the remainder populates several other residual nuclides. It is probable that continued analysis of the data will identify a significant part of these other nuclides.

RESULTS

A γ-ray singles spectrum produced by ^{40}Ca + ^{60}Ni with $E_{lab}=140$ MeV and $\theta_{lab}=135°$ is shown in Fig. 4. Several

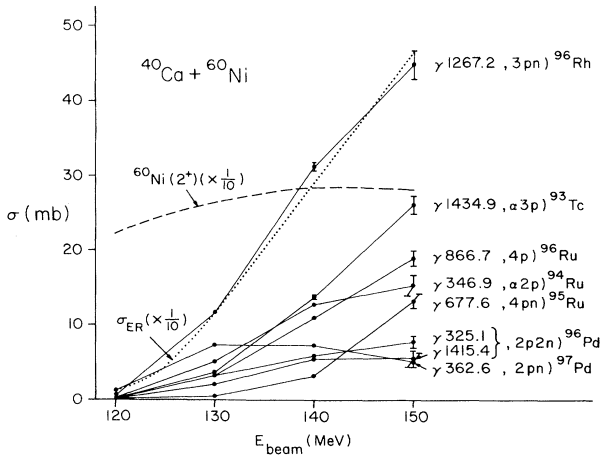

FIG. 3. The γ-ray excitation functions produced by 120-, 130-, 140-, and 150-MeV ^{40}Ca + ^{60}Ni. The data have been normalized to the calculated cross section for exciting the ^{60}Ni 2_1^+ state (the dashed curve). The γ-ray intensities have been corrected for the Ge(Li) detector efficiency and the γ-ray angular distribution. Also shown is the empirical total evaporation residue cross section (the dotted curve) of Sikora *et al.* (Ref. 18) which has been corrected for the finite ^{60}Ni target thickness ($\Delta E \simeq 14$ MeV) as discussed in the text. The 325.1- and 1415.4-keV transitions are assigned to ^{96}Pd.

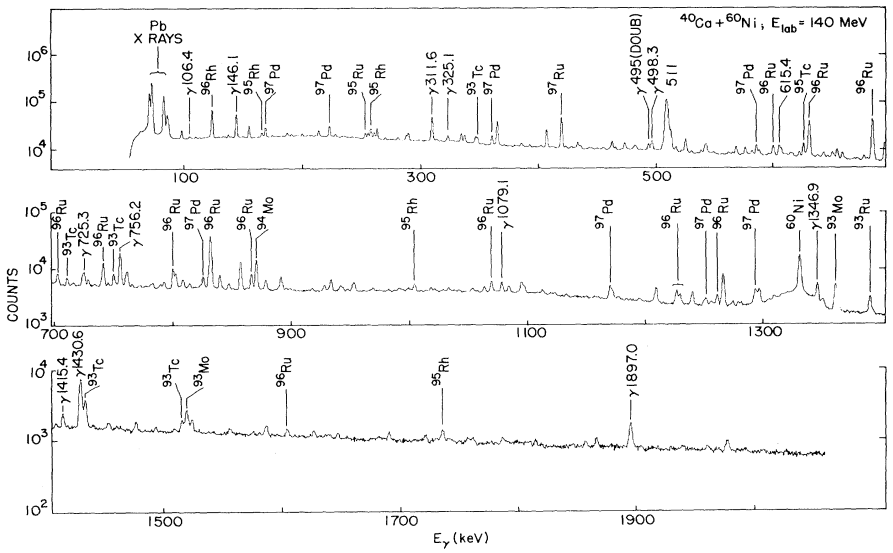

FIG. 4. A Ge(Li) γ-ray singles spectrum recorded at 135° and produced by $^{40}Ca+^{60}Ni$ with $E_{beam}=140$ MeV. The transitions assigned to ^{96}Pd and ^{94}Ru are labeled with their energies (in keV) while other transitions, identified previously, are labeled by nuclide.

transitions identified previously in ^{97}Pd, ^{95}Rh, $^{97,96,95,94,93}Ru$ and $^{95,93}Tc$ are labeled (by nuclide) along with previously unstudied ^{96}Rh whose identification is a by-product of the present work. In order to identify candidate transitions for ^{96}Pd, Fig. 5(b) shows a γ-ray spectrum gated by two neutrons. A correction has been made to this spectrum to subtract the contribution due to one neutron scattering from any one NE213 segment to another, thereby causing both to trigger. This correction was accomplished by the subtraction of a fraction f of the one-neutron gated spectrum displayed in Fig. 5(a) from the "raw" 2n-gated spectrum, yielding the spectrum displayed in Fig. 5(b). The value of $f=0.0049\pm0.0004$ was determined from the data by requiring that the transitions of ^{96}Rh, produced by

$$^{60}Ni(^{40}Ca,3pn\gamma)^{96}Rh\ ,$$

and ^{97}Pd, produced by

$$^{60}Ni(^{40}Ca,2pn\gamma)^{97}Pd\ ,$$

should not appear in the "true" 2n-gated spectrum. This value of f is in agreement with values determined from previous experiments using this array of neutron detectors.[20]

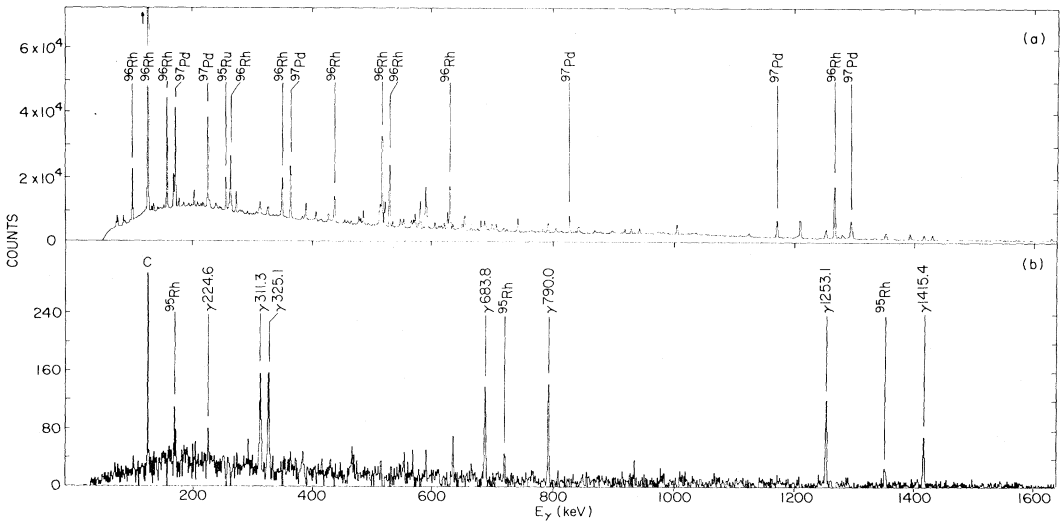

FIG. 5. Gated Ge(Li) γ-ray spectra recorded using $^{40}Ca+^{60}Ni$ with $E_{beam}=140$ MeV. (a) Spectrum gated by one neutron. Previously identified transitions are labeled by nuclide. (b) Spectrum gated by two neutrons and corrected for neutron scattering as discussed in the text. Except for three transitions previously assigned to ^{95}Rh and therefore produced by the 3p2n evaporation channel, the only peaks seen correspond to the 2p2n channel, i.e., ^{96}Pd.

Gamma-gamma coincidence gates were set on the transitions seen in Fig. 5(b), and the EMR tapes were scanned to produce gated spectra. The summed spectrum of three background-subtracted gates is shown in Fig. 6(a) and, with the additional requirement of a coincident neutron, the sum of four gates is shown in Fig. 6(b). Inspection of the individual gates allowed a level scheme for ^{96}Pd to be constructed as shown in Fig. 7. Notice in Fig. 6 that γ 224.6 appears only in the neutron-gated summed spectrum. This is an effect of the lifetime of the isomeric $J^{\pi}=8^{+}$ level; i.e., the rate of coincidence of the lower transitions with neutrons is attenuated due to the finite range (500 ns) of the n-γ time-to-amplitude converter (TAC).

Of the transitions included in the ^{96}Pd level scheme in Fig. 7, only the 1415.4-, 325.1-, 1253.1-, and 790.0-keV transitions are reasonably intense and resolved from other transitions in a γ-ray singles spectrum. In order to determine how many protons are in coincidence with these four transitions, Fig. 8 displays, for several previously identified transitions, the ratio of the background-subtracted photopeak intensity in a γ-ray spectrum gated by two protons to that in a spectrum gated by one proton. It can be seen that the value of this ratio clusters into groups corresponding to the number of evaporated protons. Transitions from the 2pn(^{97}Pd) and α2p(^{94}Ru) channels were used to calibrate the "2p" region. Therefore, the ratio found for an unassigned transition may be used to determine the number of preceding evaporated protons yielding that transition. Figure 8 also shows the empirical ratios found for the four ^{96}Pd transitions which are seen to follow the evaporation of two protons. Since we use intensity ratios, the effect of any preceding isomeric levels is canceled. From this result (and the observation that none of these four transitions is observed to be in coincidence with alpha particles) and the 2n-gated γ-ray spectrum shown in Fig. 5b, it is concluded that the four transitions are produced by the 2p2n evaporation channel. Therefore, the level scheme displayed in Fig. 7 can be assigned to ^{96}Pd. The assignment of the four most intense transitions in Fig. 7 (the intensity of the 106.4 keV transition has been corrected for a total internal conversion coefficient $\alpha=1.12$) is in agreement with that of Kurcewicz *et al.*[12] from a study of the β^{+}-EC decay of 5.1 s ^{96}Ag, produced by ^{40}Ca+^{60}Ni with $E_{\text{lab}}=160$ MeV, as mentioned above. Moreover, the

$$8^{+}\rightarrow 6^{+}\rightarrow 4^{+}\rightarrow 2^{+}\rightarrow 0^{+}$$

energy differences are similar to analogous ones in the isotones ^{90}Zr, ^{92}Mo, and ^{94}Ru. In addition, the level energies deduced for ^{96}Pd are in agreement with the expectations for a $(\pi g_{9/2})^{n}$ configuration as will be discussed below. The intensities of the ^{96}Pd transitions are summarized in Table II. The usefulness of the array of neutron detectors is apparent from Fig. 5(b) where, except for three weak ^{95}Rh transitions, the only peaks seen are those assigned to ^{96}Pd. The ^{96}Pd transitions were not found in the previous angular γ-ray distribution spectra mentioned above with sufficient intensity to obtain additional information on their multipolarity. Therefore, the spin-parity assignments shown in Fig. 7 are based on systematics and are in good agreement with the predictions of shell-model calculations.

In order to determine the lifetimes of the ^{96}Pd levels, background-subtracted γ-ray gates were set on the 1415.5-, 683.8-, 1253.1-, and 790.0- keV transitions. The two-parameter EMR tapes mentioned above were then scanned to produce the time spectra shown in Fig. 9 where the abscissae measure the time difference between a neutron and a γ ray. The other transitions of lower energy could not be utilized because of subtle effects due to the electronics. The two time spectra for γ790.0 and γ1253.1 were found to be similar so that only the summed spectrum is shown in Fig. 9(b). A fit to the data yields a half-life of 58±5 ns. Although we cannot assign this half-life to a specific level of ^{96}Pd, we remark that the delayed intensity of γ1253.1 is 7% of the total for this transition while the delayed part of γ790.0 is 12%. The two time spectra corresponding to the 1415.4- and 683.8-keV transitions were found to be similar to each other. Therefore, only the sum of these two spectra is shown in Fig. 9(a). A four parameter two-lifetime fit shown by the dotted line in

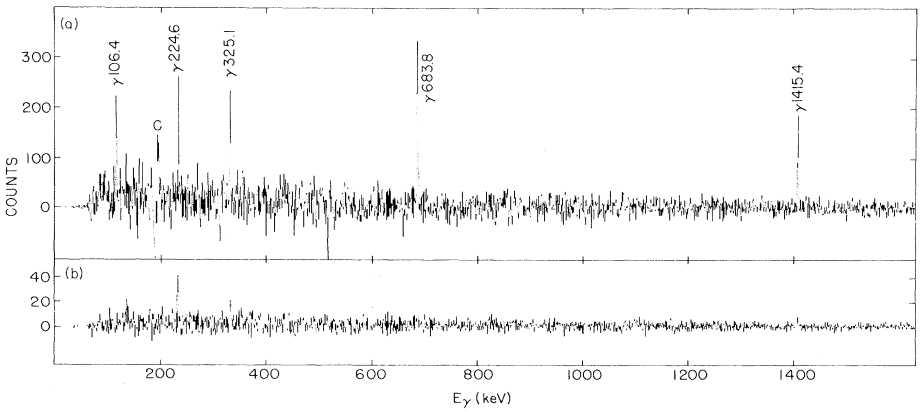

FIG. 6. (a) Sum of background-subtracted γ-γ coincidence gates on γ1415.4, γ325.1, and γ106.4 in ^{96}Pd. The γ683.8 gate contained mainly ^{96}Ru transitions and was therefore omitted. The structure labeled by a "c" is due to annihilation radiation scattering from one Ge(Li) detector to the other. (b) Sum of background-subtracted γ-γ coincidence gates on γ1415.4, γ683.3, γ325.1, and γ106.4 with the additional requirement of being gated by a neutron. In this spectrum the 224.6 keV transition, which is not attenuated by the isomeric $J^{\pi}=8^{+}$ state of ^{96}Pd is apparent.

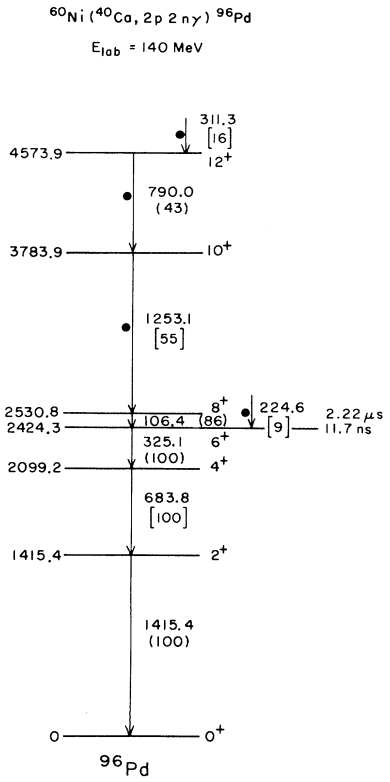

FIG. 7. Level scheme of ^{96}Pd. The relative γ-ray intensities at $\theta=135°$ corrected for Ge(Li) detector efficiency are given in parentheses while intensities determined from coincidence data are given in brackets. The 106.4 keV transition intensity has been corrected using an internal conversion coefficient $\alpha_T=1.12$. The transitions not previously reported are labeled with a black dot.

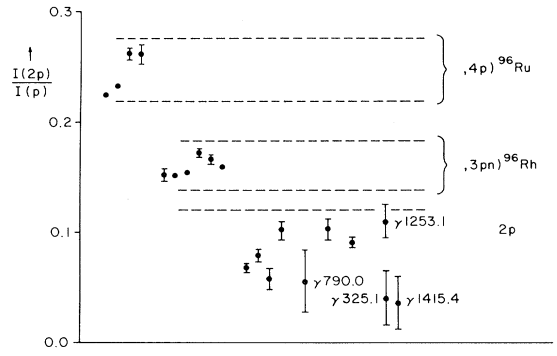

FIG. 8. For each of several previously identified transitions, the ratio of the background-subtracted γ-ray photopeak intensity in a spectrum gated by two protons to that in a spectrum gated by one proton is shown. The abscissa is not defined. The data cluster according to the preceding number of evaporated protons. Also shown are the data for the 1415.4-, 325.1-, 1253.1-, and 790.0-keV transitions. These four transitions are associated with the evaporation of exactly two protons (and two neutrons).

TABLE II. Transitions in ^{96}Pd produced by 140 MeV ^{40}Ca+^{60}Ni. The relative γ-ray intensity at 135°, corrected for the Ge(Li) detector efficiency, is listed in the second column.

Transition energy (keV)	Relative intensity	Assignment
106.45±0.20	39.8±2.9	$8^+ \rightarrow 6^+$
224.60±0.30	9.4±4.7[ae]	$\rightarrow 6^+$
311.3 ±0.4	16 ±7[be]	$\rightarrow 12^+$
325.13±0.30	103.0±3.5	$6^+ \rightarrow 4^+$
683.82±0.30	94 ±16[ce]	$4^+ \rightarrow 2^+$
790.04±0.30	43.0±4.5	$12^+ \rightarrow 10^+$
1253.1 ±0.5	55 ±12[ad]	$10^+ \rightarrow 8^+$
1415.41±0.30	≡100.0±4.1	$2^+ \rightarrow 0^+$

[a]Unresolved from a ^{97}Pd transition.
[b]Unresolved from a ^{94}Ru transition.
[c]Unresolved from a ^{96}Ru transition.
[d]Determined from 2n-gated spectra.
[e]Determined from γ-γ coincidence data.

Fig. 9(a) was found to be sufficient to describe the data where the two half-lives are 11.6 ns and 279 ns. One expects the longer half-life to be that of the $J^\pi=8^+$ state. As mentioned above, Grawe and Haas[15] have determined an 8^+ half-life of 2.22±0.28 μs from data covering a time range of about 5 μs whereas the data shown in Fig. 9 only cover a range of 250 ns. Therefore, we adopt their previous value and repeat the fit [three parameters—solid curve in Fig. 9(a)] yielding a half-life for the short component of 13.3 ns. If we interpret this half-life as being that of the 6^+ state, then the two fitted intensity parameters indicate that the $8^+ \rightarrow 6^+$ transition accounts for 84±7% of the

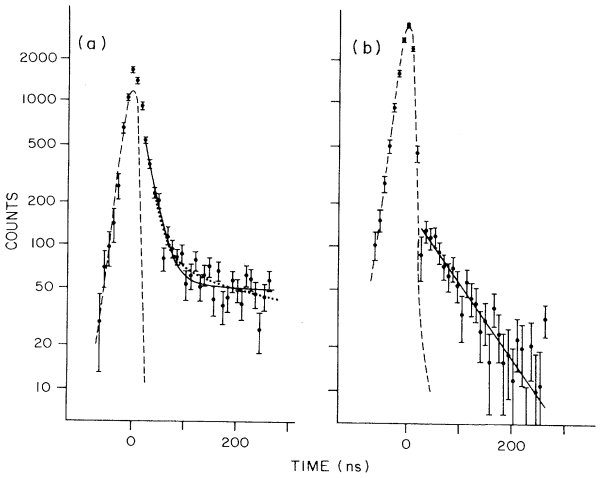

FIG. 9. (a) Sum spectrum of two background-subtracted time spectra gated by the 1415.4- and 683.8-keV transitions in ^{96}Pd. The time-to-amplitude converter was "started" by a neutron related pulse and "stopped" by a γ-ray related pulse. The "prompt" curve, determined from other transitions is shown. The two curves resulting from separate two-lifetime fits to the data are discussed in the text. (b) Summed spectrum of two background-subtracted spectra gated by the 1253.1- and 790.0-keV transitions in ^{96}Pd. A single lifetime was found to be sufficient to describe the data.

population of the 6^+ state. This is in agreement with the γ-ray intensities listed in Table II; after correcting the $8^+ \rightarrow 6^+$ transition for internal conversion, its total transition intensity is $86 \pm 7\%$. This latter half-life is to be compared with the 6^+ half-life of 4.5 ± 1.4 ns found by Grawe and Haas. In order to check the possibility that the 58 ns isomer is perturbing our value, we repeat the fit to Fig. 9(a) using four parameters and three half-lives, the larger two of which are constrained to be 58 ns and 2.22 μs. (Therefore, the four parameters involve three intensities and one half-life.) This fit yields a 6^+ half-life of 10.4 ns. All three of the fits which have been mentioned have nearly the same value of χ^2. Therefore, to allow for all possibilities, we adopt a 6^+ half-life of 11.7 ± 2.8 ns which is considerably longer than the previous result of Grawe and Haas. The origin of the disagreement is unclear. We find that, using a value of $\alpha_T = 0.0228$ for the total internal conversion coefficient, found by a double-logarithmic interpolation of the tables of Rösel *et al.*,[21] the reduced transition strength for the $6^+ \rightarrow 4^+$ transition of ^{96}Pd is

$$B(E2, 6^+ \rightarrow 4^+) = (1.30 \pm 0.32) \times 10^{-3} e^2 b^2 (0.50 \text{ W.u.}) .$$

This strength is seen in Table III to be intermediate between the analogous values found for ^{92}Mo and ^{94}Ru.

From the γ-ray excitation functions shown in Fig. 3, it is apparent that the isotone ^{94}Ru is produced intensely. Therefore, it proved feasible to deduce a level scheme for ^{94}Ru by setting γ-γ coincidence gates on the previously identified transitions of ^{94}Ru.[5,22] An inspection of the background-subtracted gated γ-ray spectra allowed the inference of two essentially separate γ-ray cascades in agreement with the level scheme proposed recently by Nolte *et al.*[5] Figure 10 shows two spectra, each of which is a sum of background-subtracted γ-γ coincidence gates for the highest-spin transitions of ^{94}Ru, in one of the two cascades. The level scheme for ^{94}Ru is displayed in Fig. 11. The lower part is in agreement with the level scheme proposed by Nolte *et al.* and, in addition, 11 new transitions are shown (identified with black dots). The relative transition intensities produced by ^{40}Ca+^{60}Ni along with the γ-ray angular distribution results obtained from two other reactions are summarized in Table IV.

TABLE III. The systematic behavior of the $B(E2, J \rightarrow J-2)$ values of the $8^+ \rightarrow 6^+$ and $6^+ \rightarrow 4^+$ transitions in the even-A $N = 50$ nuclides above ^{88}Sr.

Nuclide	J^π	$B(E2, J \rightarrow J-2)$ (W.u.)
^{90}Zr	8^+	2.5
^{92}Mo	8^+	1.3
	6^+	3.2
^{94}Ru	8^+	3.4×10^{-3}
	6^+	0.10
^{96}Pd	8^+	0.33[a]
	6^+	0.50[b]

[a]Deduced from the results of Ref. 15.
[b]This experiment.

There are (at least) two features seen in Fig. 11 which pose a challenge to understanding the nature of ^{94}Ru. First, there is the apparently repeating pattern formed by the sequence of transitions γ139.3-γ793.0-γ1113.4, γ230.0-γ495.3-γ1079.1, and γ291.6-γ539.9-γ1033.6. Second, there appears a series of γ-ray transitions: γ394.4-γ484.8-γ638.2-γ630.3-γ615.4-γ542.9. The four lowest-lying of these, which were also observed by Nolte *et al.*,[5] have recently been interpreted by Shimano *et al.*[23] as connecting states involving the excitation of a $g_{9/2}$ neutron across the $N = 50$ shell in cooperation with the six protons in the $p_{1/2}$ and $g_{9/2}$ orbitals. A comparison of the levels deduced from experiment and the calculated level energies of Shimano *et al.* is given in Fig. 12. Those calculated levels which involve the excitation of a $g_{9/2}$ neutron are indicated with a black dot. A possible association between an empirical level and a calculated level is indicated by a dashed line in Fig. 12.

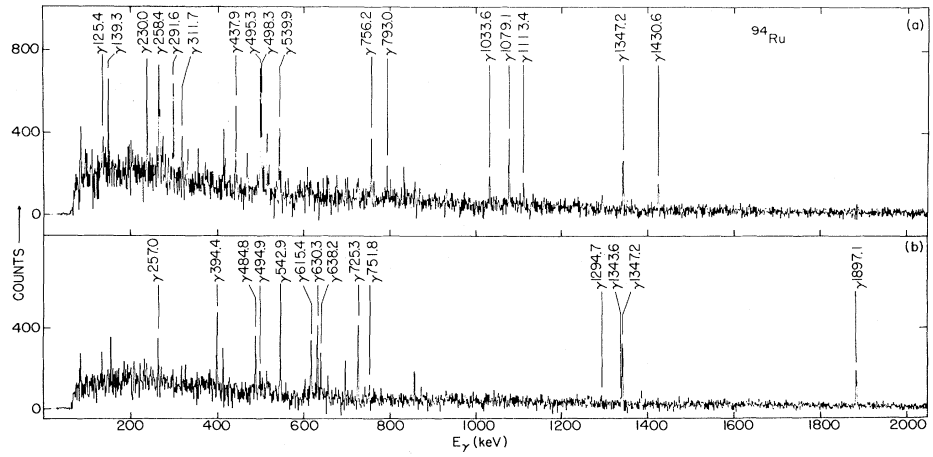

FIG. 10. Summed spectra of background-subtracted γ-γ coincidence gates set on transitions in ^{94}Ru. (a) Sum of gates on 1033.6-, 539.9-, 291.6-, 498.3-, 1079.1-, 495.3-, 230.0-, 1113.4-, 793.0-, and 139.3-keV transitions. (b) Sum of gates on 725.3-, 1897.1-, 542.9-, 1294.7-, 615.4-, 638.2-, 484.8-, and 394.4-keV transitions.

TABLE IV. Transitions in ^{94}Ru produced by 140 MeV ^{40}Ca+^{60}Ni. The relative γ-ray intensities at 135° corrected for the Ge(Li) detector efficiency are listed in the second column. The angular distribution results from two other reactions are listed as discussed in the text.

Transition energy (keV)	Relative intensity $\theta=135°$	^{35}Cl+^{66}Zn, 165 MeV A_2/A_0	^{35}Cl+^{66}Zn, 165 MeV A_4/A_0	^{32}S+^{70}Ge, 130 MeV A_2/A_0	^{32}S+^{70}Ge, 130 MeV A_4/A_0	Assignment
125.44±0.40	2	a	a	−0.23 ±0.07	+0.02 ±0.11	$5^- \rightarrow 6^+$
139.34±0.20	3.4±1.5	a	a	e	e	^{94}Ru
146.12±0.10	53.6±0.8	a	a	−0.050±0.031	+0.024±0.044	$8^+ \rightarrow 6^+$
229.96±0.25	5.3±0.6	−0.03 ±0.10	−0.15 ±0.17	e	e	^{94}Ru
256.90±0.30	1.5±0.5	d	d	d	d	$(14^- \rightarrow 13_2^-)$
258.4 ±0.4	7.4±1.4	e	e	−0.54 ±0.09	+0.33 ±0.12	^{94}Ru
291.60±0.30	5.7±0.8	e	e	−0.02 ±0.06	+0.02 ±0.09	$(11^- \rightarrow 9^-)$
311.66±0.10	92.0±1.2	+0.016±0.030	−0.117±0.049	−0.123±0.027	+0.016±0.040	$6^+ \rightarrow 4^+$
394.45±0.35	3.8±0.5	−0.13 ±0.18	−0.34 ±0.28	e	e	$(19^+ \rightarrow 18^+)$
437.89±0.25	5.7±1.0	e	e	+0.071±0.024	−0.011±0.036	$5^- \rightarrow 4^+$
484.77±0.40	4.0±1.2	e	e	e	e	$(18^+ \rightarrow 17^+)$
494.9 ±0.5	2.0±0.9	d	d	d	d	$(13_2^- \rightarrow 14^+)$
495.30±0.25	10.1±1.5	−0.35 ±0.10	+0.06 ±0.15	e	e	$\rightarrow (13^-)$
498.30±0.15	19 ±2	−0.350±0.037	+0.137±0.058	−0.14 ±0.12	−0.01 ±0.17	$(11^-) \rightarrow 10^+$
539.92±0.25	5.5±0.5	d	d	+0.28 ±0.19	−0.39 ±0.27	$(9^- \rightarrow 7^-)$
542.88±0.30	17 ±4	+0.03 ±0.09	−0.13 ±0.15	−0.13 ±0.10	+0.04 ±0.15	$(14^+ \rightarrow 13^+)$
615.38±0.35	10.4±0.6	c	c	e	e	$(15^+ \rightarrow 14^+)$
630.26±0.40	6.9±0.7	f	f	f	f	$(16^+ \rightarrow 15^+)$
638.22±0.45	5.7±0.9	−0.28 ±0.11	−0.01 ±0.17	e	e	$(17^+ \rightarrow 16^+)$
725.34±0.30	33 ±3	+0.233±0.025	−0.113±0.040	+0.319±0.012	−0.082±0.017	$12^+ \rightarrow 10^+$
751.76±0.40	3.1±1.0	d	d	e	e	$(14^- \rightarrow 14^+)$
756.25±0.20	100 ±3	+0.066±0.021	−0.063±0.033	+0.238±0.034	−0.057±0.050	$4^+ \rightarrow 2^+$
792.97±0.30	3.4±1.0	−0.19 ±0.15	−0.32 ±0.24	e	e	^{94}Ru
1033.57±0.30	3.8±0.7	e	e	e	e	$(7^-) \rightarrow 5^-$
1079.11±0.30	18.6±0.8	+0.12 ±0.07	−0.26 ±0.11	+0.01 ±0.11	+0.03 ±0.17	$(13^- \rightarrow 11^-)$
1113.4 ±0.4	5.1±0.7	e	e	e	e	^{94}Ru
1294.7 ±0.5	4.0±2.0	b	b	+0.16 ±0.09	+0.01 ±0.13	$(14^- \rightarrow 13^+)$
1343.47±0.30	4.1±1.2	+0.03 ±0.18	−0.04 ±0.29	+0.27 ±0.14	−0.29 ±0.20	$\rightarrow (14^-)$
1347.17±0.35	42 ±2	+0.297±0.033	−0.096±0.053	+0.29 ±0.10	−0.03 ±0.14	$10^+ \rightarrow 8^+$
1430.60±0.17	≡100.0±0.9	+0.160±0.043	−0.051±0.070	+0.074±0.032	−0.013±0.048	$2^+ \rightarrow 0^+$
1897.1 ±0.6	22.4±0.7	−0.29 ±0.12	+0.14 ±0.18	−0.30 ±0.22	−0.11 ±0.32	$(13^+) \rightarrow 12^+$

[a]Transition not recorded due to an electronic threshold.
[b]Unresolved from a ^{97}Pd transition.
[c]Unresolved from a calibration source transition.
[d]Unresolved from another ^{94}Ru transition.
[e]Unresolved from another transition.
[f]Unresolved from a ^{96}Ru transition.

DISCUSSION

There have been over the years several calculations of the level energies and electromagnetic properties of the $N=50$ nuclides of which we shall mention four of the most recent. The calculations of Gloeckner and Serduke[9] mentioned above described the $N=50$ nuclides from ^{90}Zr to ^{95}Rh as an inert ^{88}Sr core plus an appropriate number of valence protons. An effective interaction was extracted from an eleven parameter fit to the energies of 45 nuclear levels and the measured transition strengths. An important constraint on the extracted parameters was the unusually retarded $B(E2)$ value of 3.4×10^{-3} W.u. for the $8^+\rightarrow6^+$ transition in ^{94}Ru. Gloeckner and Serduke were able to explain this transition rate as an effect of seniority mixing in the $(p_{1/2},g_{9/2})$ model space, although contributions from outside of the model space could not be excluded. Amusa and Lawson have recently reported a detailed comparison[6] of their shell-model calculations for the valence protons to the empirical results for ^{94}Ru and ^{95}Rh. The overall agreement seems good except for an expected $9^-\rightarrow8^+$ transition in ^{94}Ru which has not been found in the data. An inspection of a γ-ray singles spectrum allows an upper limit to be set for the relative intensity that is 2% of the ^{94}Ru $2^+\rightarrow0^+$ transition. This yields a $9^-\rightarrow8^+$ transition strength which is empirically at least 45 times weaker, relative to the $9^-\rightarrow7^-$ one, than the calculated strength. This reduction of the reduced electric dipole strength may be due to minor components in the wave functions for the $J^\pi=9^-$ and 8^+ states. Strottman[7] has recently calculated the spectra of ^{94}Ru and ^{96}Pd without adjusting parameters by considering protons in the $f_{5/2}$, $p_{3/2}$, $p_{1/2}$, and $g_{9/2}$ orbitals. The highest spin attained in the model space of all three of these calculations[6–8] is $J^\pi=13^-$ (12^+ for ^{96}Pd). Most recently Shimano *et al.*[23] have, in addition, considered the excitation of a $g_{9/2}$ neutron as mentioned above. The comparison of their calculated levels of ^{94}Ru with the empirically deduced levels

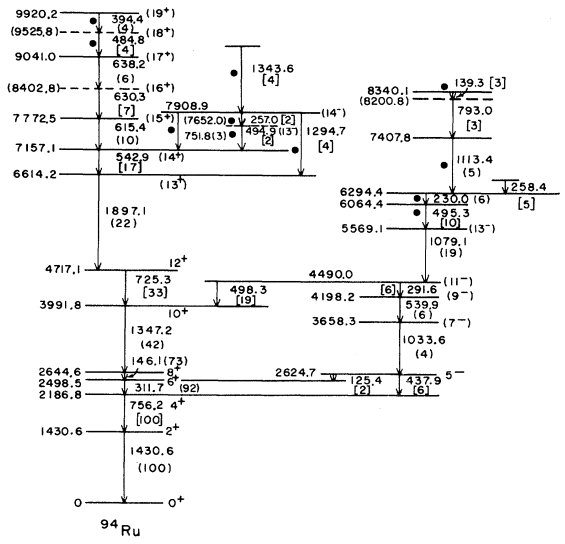

FIG. 11. Level scheme of ^{94}Ru deduced from the present work. The relative transition intensities, corrected for Ge(Li) detector efficiency, are shown in parentheses if determined from a singles spectrum or in square brackets if better determined from coincidence spectra. The new transitions are indicated by a black dot. The lower part of the level scheme is in agreement with the previous work.

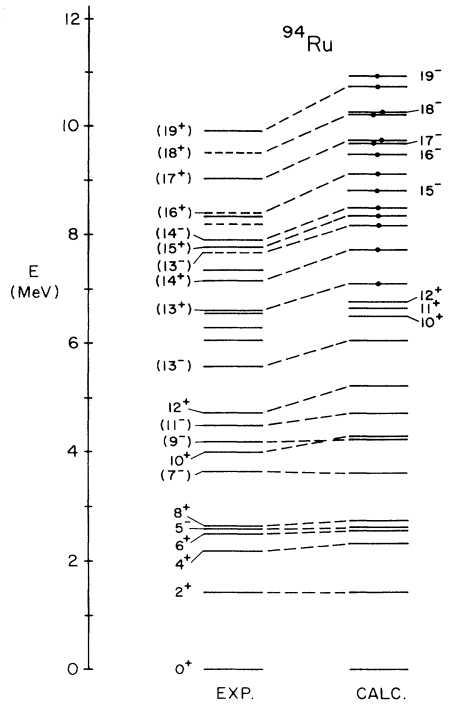

FIG. 12. A comparison of the levels deduced from the present data with the levels calculated by Shimano *et al.* (Ref. 23). Those calculated levels which involve the excitation of a $g_{9/2}$ neutron across the $N=50$ shell closure into a $d_{5/2}$ orbital are indicated by a black dot.

shown in Fig. 12 suggests that levels involving the neutron excitation have been populated. It will be interesting to find evidence in future experiments for the neutron states in the higher-spin states of ^{96}Pd.

To sum up, the yrast states of ^{96}Pd have been identified up to the $J^\pi=12^+$ state. The lower-spin states up to $J^\pi=8^+$ are in agreement with those reported recently by two separate groups. The energy spacings were found to be nearly those expected from both shell-model calculations and from the systematic behavior of the lighter $N=50$ isotones. Moreover, the half-life of the $J^\pi=6^+$ state has been measured and found to be longer than reported previously. The corresponding reduced electric quadrupole transition intensity is between the analogous strengths in the isotones ^{92}Mo and ^{94}Ru. Finally, new high-spin states of ^{94}Ru have been deduced and evidence for $g_{9/2}$ neutron excitations across the $N=50$ shell closure possibly has been found.

ACKNOWLEDGMENTS

We would like to thank Dr. A. H. Lumpkin, Professor J. J. Kolata, Dr. H. Morinaga, and Dr. W. Dünnweber for their interest in the early phases of this work. This work was supported in part by the U. S. DOE under contract DE-AC02-76CH00016, by the NSF, and by the United Kingdom S.E.R.C.

[1]S. Cochavi, O. Kistner, M. McKeown, and G. Scharff-Goldhaber, J. Phys. 33, 103 (1972).
[2]W. F. Piel, Jr., G. Scharff-Goldhaber, A. H. Lumpkin, Y. K. Lee, and D. C. Stromswold, Phys. Rev. C 23, 708 (1981).
[3]W. F. Piel, Jr., and G. Scharff-Goldhaber, Bull. Am. Phys. Soc. 23, 555 (1978).
[4]W. F. Piel, Jr., and G. Scharff-Goldhaber, Phys. Rev. C 15, 287 (1977).
[5]E. Nolte, G. Korschinek, and U. Heim, Z. Phys. A 298, 191 (1980).
[6]A. Amusa and R. D. Lawson, Z. Phys. A 307, 333 (1982).
[7]D. Strottman, private communication.
[8]N. Auerbach, private communication.
[9]D. H. Gloeckner, M. H. MacFarlane, R. D. Lawson, and F. J. D. Serduke, Phys. Lett. 40B, 597 (1972); D. H. Gloeckner and F. J. D. Serduke, Nucl. Phys. A220, 477 (1974).
[10]W. F. Piel, Jr., J. J. Kolata, A. H. Lumpkin, and G. Scharff-Goldhaber, Bull. Am. Phys. Soc. 19, 474 (1974).
[11]B. A. Brown, D. B. Fossan, P. M. S. Lesser, A. R. Poletti, Bull. Am. Phys. Soc. 18, 1417 (1973); Phys. Rev. C 13, 1194 (1976).
[12]W. Kurcewicz, E. F. Zganjar, R. Kirchner, O. Klepper, E. Roeckl, P. Komninos, E. Nolte, D. Schardt, and P. Tidemand-Petersson, Gesellschaft für Schwerionenforschung Report No. GSI-82-15, 1982 (unpublished).
[13]G. Scharff-Goldhaber, in the Proceedings of the 1982 Institute for Nuclear Studies International Symposium on the Dynamics of Nuclear Collective Motion (unpublished), p. 365.

[14]C. J. Lister, B. J. Varley, W. F. Piel, Jr., and G. Scharff-Goldhaber, Bull. Am. Phys. Soc. 27, 727 (1982).
[15]H. Grawe and H. Haas, Hahn-Meitner Institute Report No. HMI-P 82/13 HF, 1982 (unpublished).
[16]N. K. Aras, P. W. Gallagher, and W. B. Walters, J. Phys. G 6, L195 (1980).
[17]W. Scobel, J. Bisplinghoff, M. Blann, A. Mignerey, P. David, J. Ernst, and T. Mayer-Kuckuk, Z. Phys. A 284, 343 (1978).
[18]B. Sikora, J. Bisplinghoff, W. Scobel, M. Beckerman, and M. Blann, Phys. Rev. C 20, 2219 (1979).
[19]F. Pühlhofer (unpublished).
[20]C. J. Lister, B. J. Varley, H. G. Price, and J. W. Olness, Phys. Rev. Lett. 49, 308 (1982).
[21]F. Rösel, H. M. Fries, K. Alder, and H. C. Pauli, At. Data Nucl. Data Tables 21, 91 (1978).
[22]C. M. Lederer, J. M. Jaklevic, and J. M. Hollander, Nucl. Phys. A169, 449 (1971).
[23]T. Shimano, K. Muto, and H. Horie, Ref. 13, p. 519.